Large Format Cross Strip Readout Image Sensors for High Temporal Resolution Astronomy and Remote Sensing

Oswald H. W. Siegmund, John V. Vallerga, Jason B. McPhate, Travis Curtis, Nate Darling,
Space Sciences Laboratory, U.C. Berkeley
Camden Ertley, Till Cremer, Alexey Lyashenko, Michael J. Minot
Incom Inc., Charlton, MA
Gary Varner
University of Hawai'i, Honolulu, Hawai'i

ABSTRACT

Microchannel Plate (MCP) detectors combine high spatial resolution (<20 μm FWHM), photon counting (noiseless) imaging in a robust, radiation-hard package that is scalable to very large formats (>10 cm & > 4k x 4k pixels). They operate at room temperature with very low dark count rate and provide event timing at the level of 10 ps. Advances in MCP technology offer potential performance improvements in quantum efficiency, long term stability, environmental stability, image quality and spatial resolution. These are being realized with cross strip (XS) readout techniques and high performance encoding electronics in concert with atomic layer deposited (ALD) microchannel plate technologies. Specific objectives are to make sensors with large areas (up to 400 cm^2) with spatial resolutions of <20 μm FWHM and timing resolutions of <100 ps for dynamic imaging. Photocathodes for the UV and visible regimes are being investigated which also allow reduction of the red response of classical multialkali photocathodes. Borosilicate MCPs processed with ALD techniques are providing large formats (20 cm) with reduced background levels, improved image fidelity and uniformity. High resolution cross strip anodes and electronics for 50mm and 100 mm detectors have been demonstrated and high-performance ASIC versions of the electronics are in development. Planacon sealed tube devices with 50 mm format provide a good test vehicle for ALD MCPs and XS anodes are already showing promising results.

Keywords: Microchannel plate, sealed tube, photon counting, imaging, timing.

1. INTRODUCTION

Photon counting detectors with high time resolution (<1ns) have been developed to cover a wide range of optical/UV sensing applications. Specifically, electronic readout microchannel plate (MCP) based sensors have been used as photon counting, imaging, event time tagging detectors for astronomical [1]-[3], remote sensing [4], time resolved biological imaging [5], imaging LIDAR and night time sensing applications [6]. They also have applications in detection of Cherenkov light (RICH) [7, 8], scintillation detection, and neutron imaging applications.

Most of the high time resolution devices to date have been relatively small format low spatial resolution devices. However, novel MCPs made by ALD on borosilicate micro-capillary arrays [8] coupled to cross strip readout anodes can potentially provide a high spatial resolution image encoding sealed tube sensors for very large formats (20 cm). ALD MCPs have shown low intrinsic background [9](<0.05 events cm^{-2} s^{-1}), and good gain stability over extended usage [10]. Optimized solar blind and FUV multialkali photocathodes show considerable promise for large area sensing in sealed tubes [11]. In concert with these developments we have made progress towards large area cross strip (XS) image readout anodes and electronics [12] to enable high spatial resolution, timing and enhanced event rates.

2. SEALED TUBE MICROCHANNEL PLATE DETECTORS

Sealed tube MCP detectors have provided a valuable platform for high time resolution photon counting imaging detectors in a number of applications [1, 3-5]. For future initiatives, the use of larger area ALD MCPs and high resolution XS readouts are being evaluated [13]. The Photonis Planacon [14] is a useful sealed detector format (~50 mm active area) to test basic functional parameters of novel technologies. These include photocathodes, MCPs and readout developments. Planacons with an anode pad array (16 x 16), two 20 μm pore ALD MCPs with 60:1 l/d and 12° pore bias and a conventional bialkali cathode have been built (Fig. 1) as a first step towards a high-resolution imaging device. The final design scheme proposed is a MgF_2 window with a narrow (200 μm) gap to the MCP surface, a pair of 10 μm pore ALD MCPs and a cross strip anode readout (Figs. 2, 3). A semitransparent photocathode can be applied to the window, and an

opaque photocathode can be deposited directly onto the MCP surface. The ALD MCP pair provides electron gain of the order 10^6 with tight single photon amplitude distribution and low background noise.

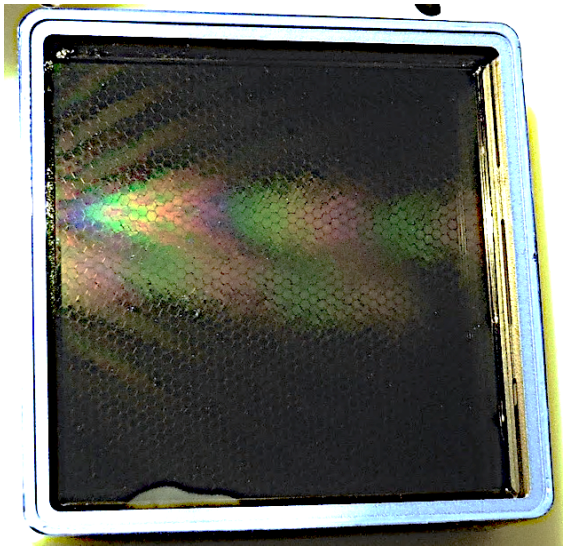

Fig. 1: Planacon 50 mm detector with a bialkali cathode and a pair of 53 mm, 20 µm pore, 60:1 L/d, 12° bias ALD borosilicate MCPs, and 16 x 16 anode pad array.

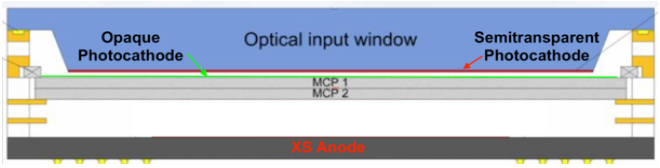

Fig. 2**:** Cross section of a cross strip Planacon sensor. The input window is MgF_2, coated with a multialkali cathode. A pair of ALD MCPs provides signal amplification and a XS anode encodes photon event positions.

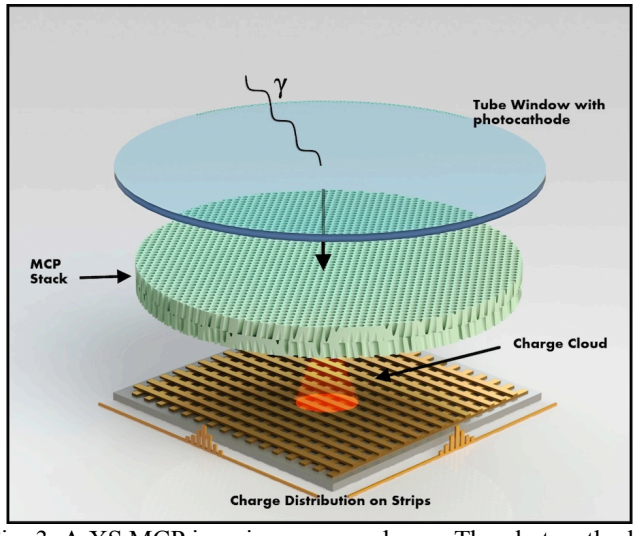

Fig. 3. A XS MCP imaging sensor scheme. The photocathode is deposited on a window facing a pair of MCPs. Emitted photo -electrons are detected by the MCPs, multiplied and sensed by several strips in each axis of an anode to encode positions.

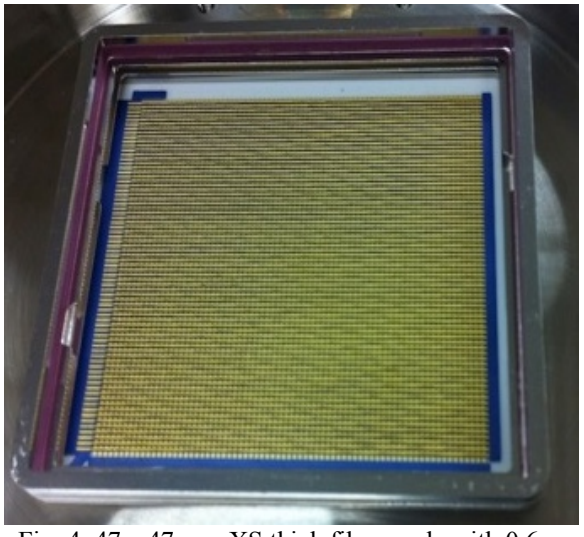

Fig. 4. 47 x 47 mm XS thick film anode with 0.6 mm strip period mounted into a Planacon style ceramic body. MCPs are placed ~2.5 mm above the anode and the window is sealed to the periphery of the body.

The XS anode is composed of layers of metals and insulators on an insulating substrate (Fig. 4). There are two sets of strips in orthogonal directions. The top and bottom layers have equal exposed areas and collect the charge from the MCPs with equal charge sharing (Fig. 3). The distance between the anode and the MCP pair is typically 2.5 mm, and is optimized for the charge cloud to spread over several periods of the XS anode (Figs. 3, 4). Each anode strip is connected to the air side of the anode hermetically allowing mounting of all the detector electronics outside the vacuum. Ceramics are used for the substrates and insulating layers [15], and the 47mm XS example a thick film process that leaves the bottom strips 50% exposed (Fig. 5). Event encoding electronics that calculates the X and Y event centroids consists of front end amplifiers for the anode signals followed by analog to digital converters and an FPGA firmware based centroid algorithm. The 47mm field of view XS anode achieves resolution of ~20 µm FHWM [15] with good image linearity in "open face" MCP detector systems.

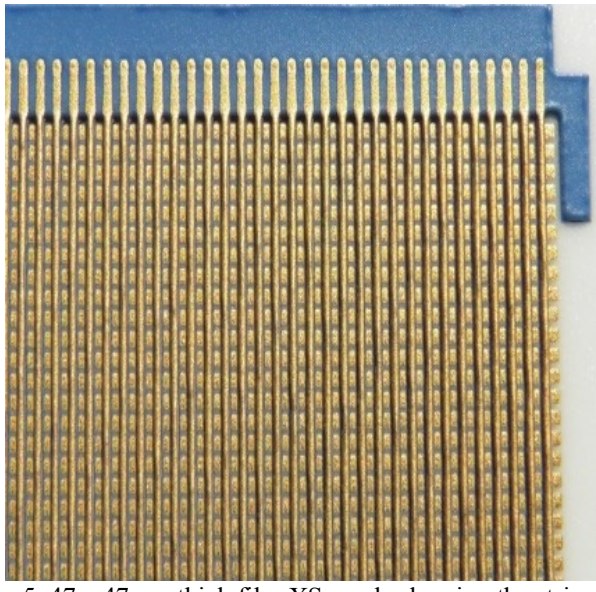

Fig. 5. 47 x 47mm thick film XS anode showing the strips in each orthogonal axis insulated from each other with ceramic stripes. 50% of the charge is captured by each axis and is spread over several strip periods [15].

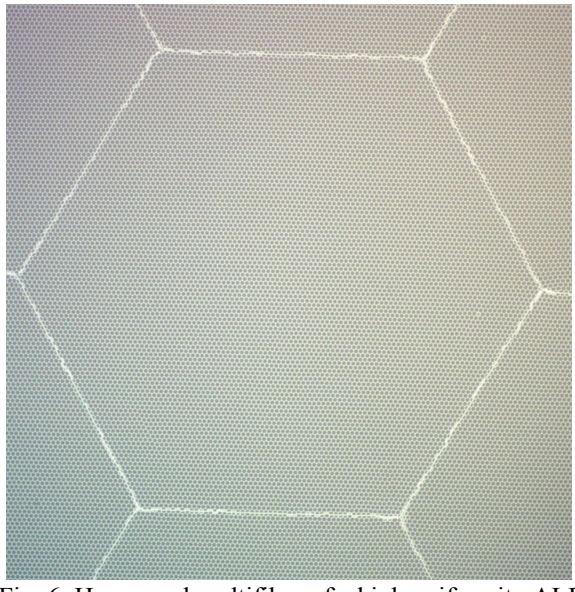

Fig. 6. Hexagonal multifiber of a high uniformity ALD MCP borosilicate substrate with 10 µm pores, 60:1 L/d, 13 ° bias. Pore crushing at the hexagonal boundary is reduced, lowering the final imaging modulations.

3. ALD MICROCHANNEL PLATES

3.1 ALD Microchannel Plate Fabrication

Atomic layer deposited MCP fabrication begins with stacking of glass tubes that are then fused together. The final MCPs show hexagonal structures (multifibers, Fig. 6) which are the fundamental stacking blocks for the glass tubes. Many multifibers are fused together to make a full size MCP. A uniform resistive layer applied by ALD provides the electrical continuity to apply a voltage across the MCP to supply the multiplication current. A secondary emissive layer is also deposited over every surface of the substrate using Al_2O_3 and MgO to achieve high secondary emission coefficient electron multiplication layers. Lastly evaporation of NiCr electrodes completes the MCP construction process.

Pore sizes of 20 µm and 10 µm are commonly available, although 6 µm [13] pore MCPs have been successfully made. The pore bias angle is either 8° or 13 °, and the pore open area ratio is typically ~74%. The resistance of MCPs can be from kΩ to GΩ. MCPs with formats of 33 mm, 46 mm circular, and 53.5 mm, 110 mm, and 203 mm square have been made and tested. Sealed tube detectors have also been made with 33 mm, 53.5mm and 203 mm MCP formats. Curved surface ALD MCPs, achieved by thermal slumping of the glass substrates, have been successfully demonstrated [13].
The robustness of MCPs using borosilicate microcapillary arrays is excellent, enabling the implementation of larger, more stable detectors for Astronomy and remote sensing. Very large focal plane areas were previously unattainable, however, recently several large format detectors have been implemented, including a 20 cm format ALD MCP detector with cross delay line image readout was successfully flown on a sub-orbital experiment twice [16] with no adverse effects.

Improvements to the construction of the ALD MCPs and their substrates are also in progress to address performance issues such as the imaging uniformity and linearity. For example some of the glass tubes (pores) at the hexagonal interfaces deform (Fig. 6) in boule fusion and result in hexagonal modulation of the images taken with detector systems (Figs. 7, 8). The pore sizes can also vary from the center of the hexagonal multifiber to the edges creating image effects. Recent efforts to improve these issues have resulted in substantial enhancements of the imaging quality of ALD MCPs. Other factors include continuing efforts to optimize the ALD secondary emissive layers to enhance the gain uniformity and stability of the gain over time and usage.

3.2 Performance of ALD Microchannel Plates

Tests with large format 53.5 mm and 100 mm ALD MCPs on borosilicate substrates in imaging detectors have demonstrated [13] many of their operational characteristics . For such large area format MCPs there are often issues with the spatial uniformity [10] due to intrinsic variations in the amplification process, and the physical flatness of the MCPs. The borosilicate substrates show good flatness, and the ALD emissive layers have achieved exceptional gain uniformity (15% [9]) over 20 cm MCPs. Images for 10 cm and 20 cm ALD MCPs clearly show the modulation of the multifibers in the MCP substrate. This modulation has been significant (50%) for early substrates but has improved as the construction

techniques have been refined. High resolution XS readout images obtained with borosilicate 10 µm pore ALD MCP pairs show hexagonal modulation, variations of response across the multifibers and the incidence of "triple point" voids has been greatly improved (Fig. 7). Detailed examination of the imaging data show modulations from both the top and bottom MCP of the pair (Fig. 8). The level of modulation is shown by the histograms in Fig. 9, with the front MCP being ~20% and the back MCP having ~12%. The response is quite flat between these hexagonal boundary areas indicating that the MCP pores are quite uniform in size. The spatial resolution is ~18 µm FWHM for the XS detector system used, which is approximately the same as the hexagonal boundary image width (Fig. 9) for the second MCP. The top MCP hexagonal boundary image width is ~25 µm and is attributable to the increased blocking of the incoming signal by the distorted MCP pores along the hexagonal boundary (Fig. 6).

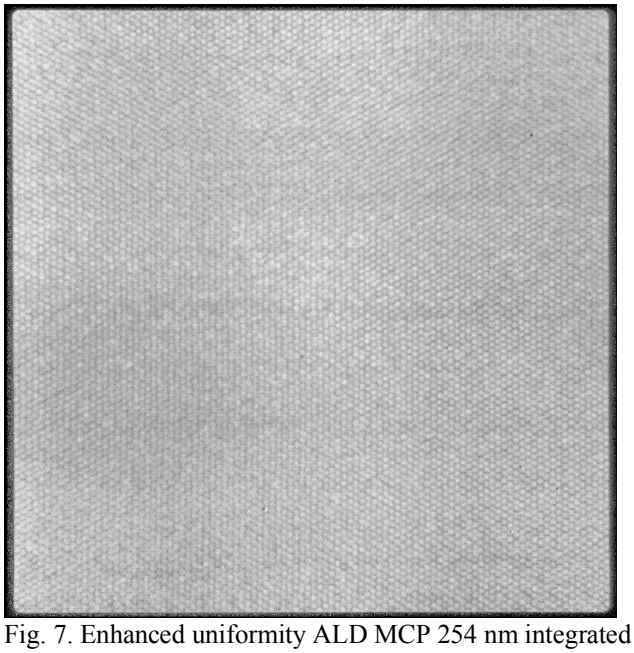

Fig. 7. Enhanced uniformity ALD MCP 254 nm integrated image using a XS readout. MCP pair, 100 mm square, 60:1 L/d, 10µm pore, 13° bias, MgO emissive layer. 25µm gap between MCP pair.

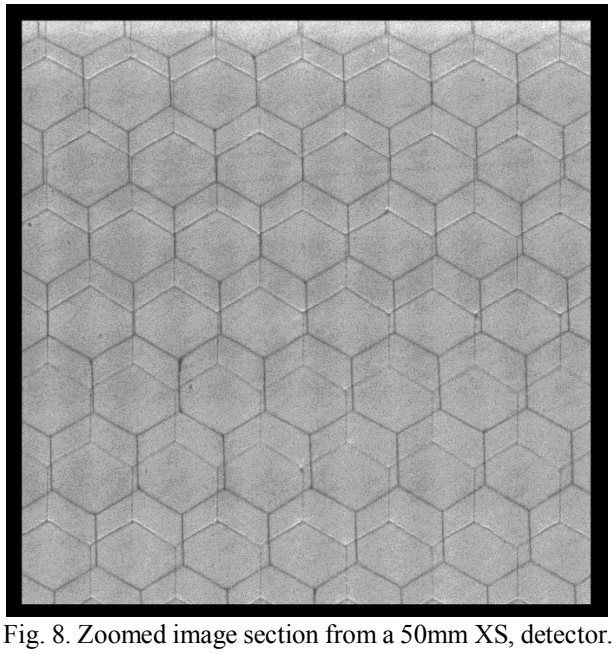

Fig. 8. Zoomed image section from a 50mm XS, detector. 60:1 L/d, 10µm pore, 13° bias, MgO ALD MCP pair, ~6 µm pixels. Shows reduced hexagonal modulation by using the most recent borosilicate substrates (Fig. 6).

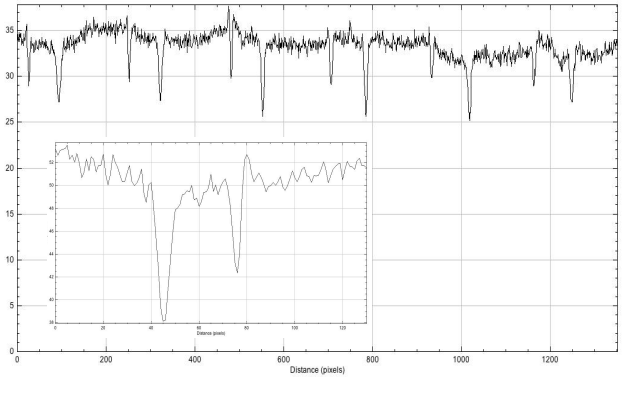

Fig. 9. Histograms of the multifiber modulation in Fig. 8. Image modulation from the front MCP is ~20% and the back is ~12%. Spatial resolution is ~18 µm FWHM (Inset).

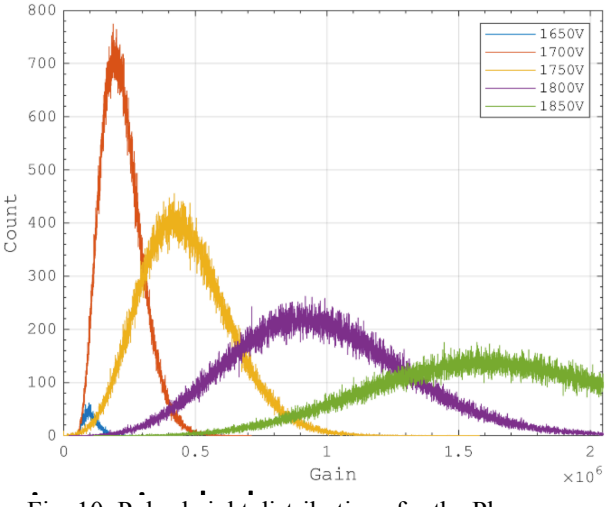

Fig. 10: Pulse height distributions for the Planacon detector shown in Fig.1. After sealed tube processing the distributions are narrow even for low gain operation.

For ALD MCPs in general we see narrower pulse amplitude distributions [17] than comparable conventional MCPs due to the high secondary emission ALD coatings. This is the case both for small and large format MCPs, and we have

seen good pulse amplitude distributions for the new sealed Planacon tubes with ALD MCPs (Fig. 10). The smaller range in pulse amplitudes reduces the dynamic range needed for electronics in new high-resolution readouts like the XS.

The processing of sealed tubes includes a preconditioning burn-in step which in conventional MCPs causes the gain of a pair to drop by one to two orders of magnitude. Recent tests of MgO coated ALD MCPs shows that the gain degrades less than a factor of two [17] for ~1 C cm^{-2} extraction during burn-in. This is also the case for the two Planacons recently made with 20 µm pore ALD MCPs, where the gain changed by about a factor of two during the sealed tube processing and preconditioning [18].

In sealed tubes the background event rate is usually dominated by the photocathode thermionic photoelectron emission. The conventional MCP intrinsic background event rate [13] is usually determined by ^{40}K beta decay resulting in ~0.3 events cm^{-2} s^{-1}. The very low ^{40}K in the ALD borosilicate substrate results in these MCPs having background rates [13] that are far lower (<0.05 events cm^{-2} s^{-1}). Also the background event spatial distribution is uniform, even for MCPs of 20 cm format [9]. Although he background would be normally dominated by the cathode noise that is not the case for sealed tubes where alkali halide opaque cathodes are deposited onto the top MCP. These cathodes have negligible noise events and would benefit from the reduced ALD MCP background event rate.

4. PHOTOCATHODES FOR SEALED TUBES

The environmental sensitivity of photocathodes that operate beyond 200 nm necessitate high vacuum sealed tube devices. Traditional visible sensitive photocathodes like bialkali (Na_2KSb) have ~30% peak at 350 nm but also show high (30%) QE in the UV [19,20] that has not been generally exploited for UV sensors. Fig. 11 shows the response curves for bialkali photocathodes on sapphire windows in Planacons. All show the 350 nm peak and the 180 nm peak. We are using this and extending bialkali cathodes into the FUV with MgF_2 windows on the next Planacon devices being made. Our recent work (Fig. 12) has made progress on optimizing the FUV bialkali QE while instituting a sharp red end cutoff.

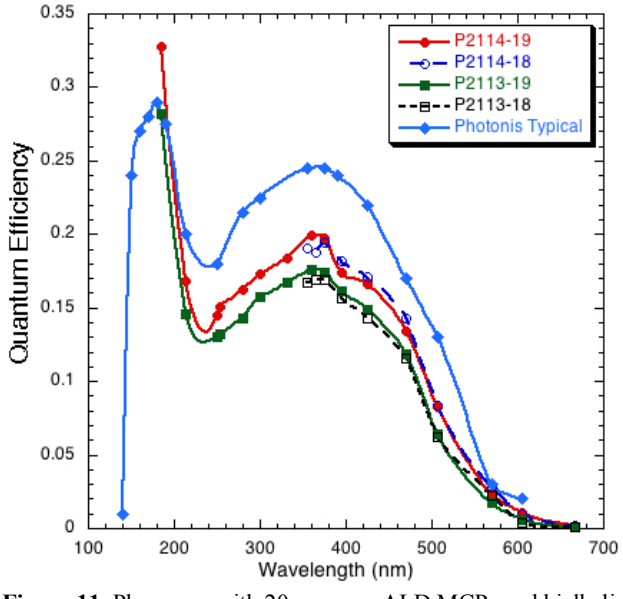

Figure 11. Planacons with 20 µm pore ALD MCPs and bialkali semitransparent photocathodes show stability over a one year time frame (2018-2019). The Al_2O_3 windows allow UV response to <180 nm and shows a 30% peak there.

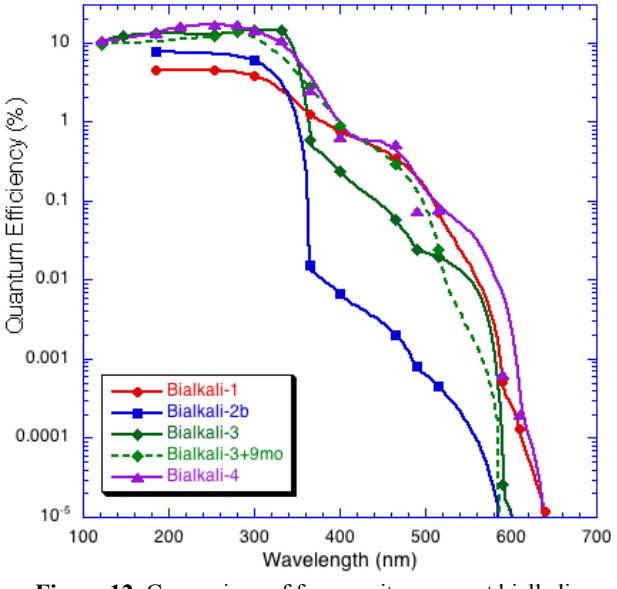

Figure 12. Comparison of four semitransparent bialkali photocathodes deposited onto MgF_2 windows. Depositions were adjusted to preserve the UV QE and minimize the response above 350nm.

The <350 nm quantum efficiency has been gradually improved, while the >350nm quantum efficiency drops off (Fig.12) far more rapidly than a conventional bialkali photocathode. Optimization of the effective work function and photoelectron escape depth is ongoing with the goal of further increasing the FUV efficiency without increasing the red end response. These photocathodes are ~25mm in size now but we expect that we can implement large area (20 × 20 cm^2) bialkali photocathodes of this kind based on our successes [21] making uniform 20 x 20 cm bialkali photocathodes with ~25% QE at 370 nm [8]). At shorter wavelengths Alkali halide (CsI, KBr) opaque photocathodes deposited directly on MCPs (Fig. 13) obtain high QE [13]. The latest 10 µm pore ALD MCPs have ~50% QE @ ~115 nm (1 photoelectron) and 65 nm (2 photoelectrons) and have broad band sensitivity from 10 nm to 180 nm.

The timing characteristics for fast pulse events in sealed tubes is usually set by the variations in ballistic trajectories of photoelectrons emitted by the photocathode as they are accelerated across to the MCPs. For single photoelectrons and narrow (200 µm) gaps the timing jitter can be as low as 45ps FWHM. The planacon proximity gap for the tubes tested is

~4.5mm so the timing jitter is proportionally greater. Fig. 14 shows the timing performance for single photon events and ~20 photoelectron pulses at different window-MCP gap potentials. The best ~80 ps timing jitter even at 700v gap potential is indicative of the large Planacon window gap. Future devices will employ narrow proximity gap windows to improve the timing jitter substantially at low gap voltages [21].

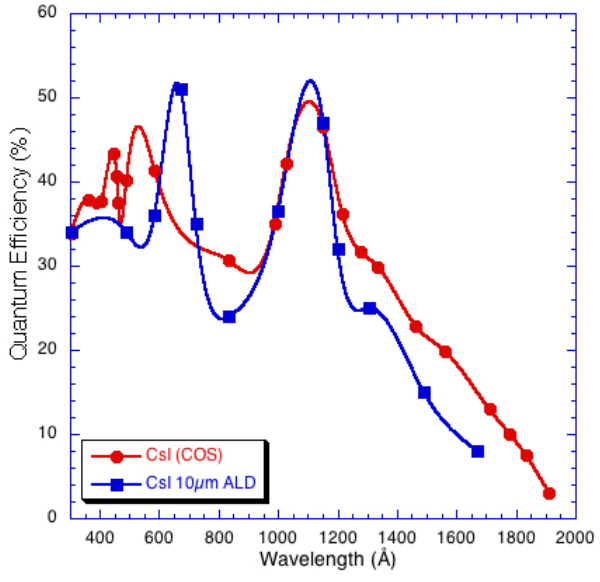

Fig 13. UV QE for an opaque CsI coated MgO ALD MCP with 67% open area, 10 µm pores, 60:1 l/d, 12° bias, compared to the opaque CsI coated MCPs (12µm pores, 19° bias, 80:1 L/d) used for the HST-COS[24] instrument.

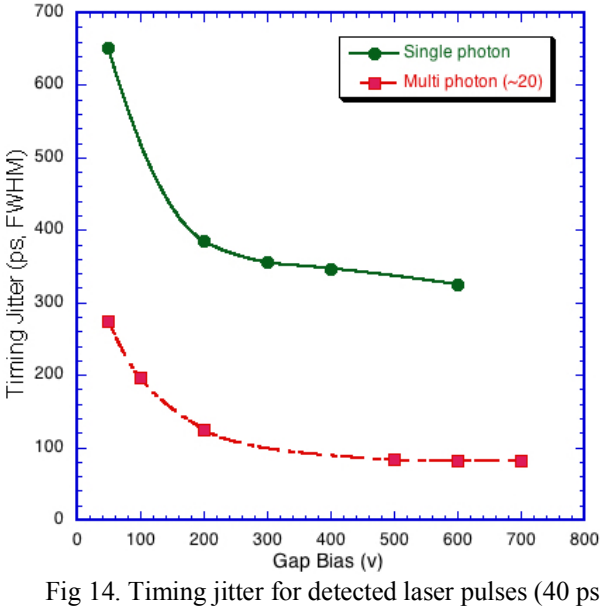

Fig 14. Timing jitter for detected laser pulses (40 ps laser @ 610 nm, 10 kHz), ALD MCP Planacon detector with 20 µm pore ALD MCP pair and bialkali cathode (gap ~4.5 mm).

5. CROSS STRIP PHOTON COUNTING IMAGING READOUT ELECTRONICS

The photon (or pulse) event position can be determined by finding the centroid of the electron charge cloud distribution spread over adjacent strips of the XS anode. Preamplifier electronics are connected at the back side of the anode close to the signal vias to achieve the best noise characteristics (lower capacitance). The anode strip period is typically ~0.65 mm, which defines the number of amplifier channels needed for a given sized detector area. Formats of 18 mm, 25mm, 50 mm and 100 mm have been implemented in the last few years using the PXS-II electronics scheme. The PXS-II [13] XS readout electronics connects each strip on the anode to a preamp input of a 32-channel ASIC(s) [12]. The output of these preamps are unipolar pulses with~50 ns rise time, ~500 ns fall time and noise of ~1000 electrons rms. The outputs for all strip signals are post-amplified before being continuously digitized by parallel 12-bit analog to digital converters operating at 50 mega-samples per second. The digital sample stream is processed by an FPGA (Xilinx Virtex6 family) to extract pulse peak information and derive the event centroid for both X and Y axes. The event centroid position is combined with a timing stamp determined from a fast amplifier and discriminator connected to the MCP output stage. The events are transmitted as an event list of X, Y (≤ 14 bits each) and T (with ~20 ps LSB). These have demonstrated resolutions of 18 µm with 50 mm XS anodes (Fig. 5, 6) and 100 mm XS anodes with event rate handling of 5 MHz at <20% deadtime [13].

A new generation of spaceflight capable electronics is currently under development as ASIC implementations with improved rate limits, and lower power and volume [12] become available. The first set of 16 channel ASICs separated the analog amplification and the digitization into separate ASICs ("CSAv3" (Fig. 15) and "HalfGraph" respectively). The CSAv3 was designed to preserve the noise performance of the preceding ASIC preamp but to speed up the recovery time to 75ns, thus permitting higher event handing rates without pileup. These two ASICs were incorporated into an 80 x 80 cross strip electronic readout using 10 ASICs of each type and controlled by two ARTIX-7 FPGAs (Fig 16). A new 16 channel ASIC that combines both the analog amplifiers and digitizers in a single 130nm CMOS process is called the GRAPH chip ("Gigasample Recorder of Analog waveforms for Photodetectors). The combination chip will save significant printed circuit board space with decreased complexity. The GRAPH chip has been fabricated and is undergoing initial performance tests.

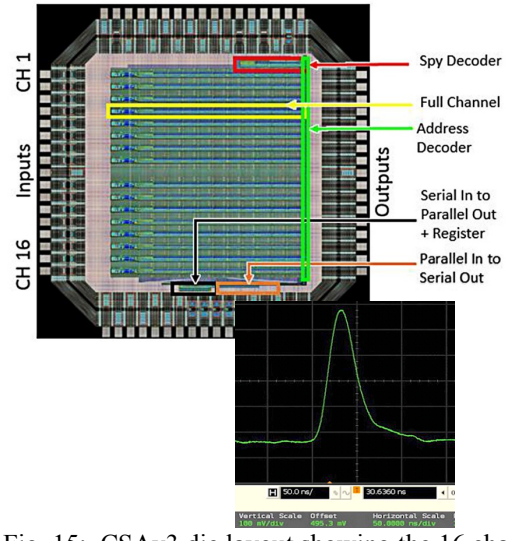

Fig. 15: CSAv3 die layout showing the 16 channels. Amplifier response to 50-fC input pulse with a 5-pF load. Note the 20-ns rise time and a return to baseline in 75 ns while retaining a noise value of ~1000 e⁻ rms.

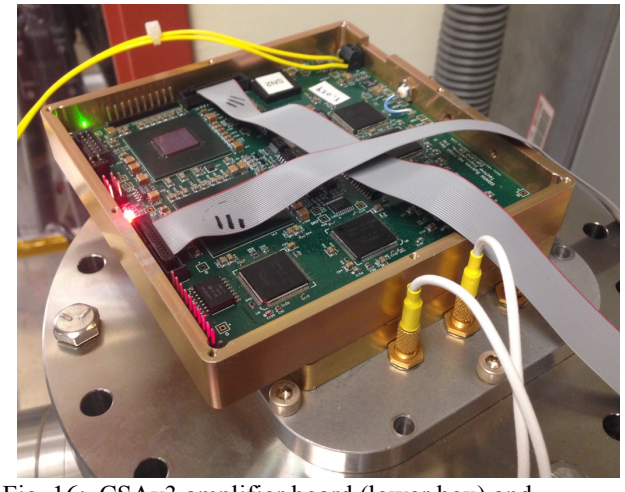

Fig. 16: CSAv3 amplifier board (lower box) and halfgraph digitizer board (upper box) mounted to a 50mm format cross strip detector.

6. LARGE AREA SEALED TUBES WITH ALD MCPS

The availability of ALD MCPs in 20 cm format enables extremely large sealed tube devices to be envisaged. Incom Inc. have successfully made such sealed tubes with ALD MCP pairs in 20 cm format (Fig. 17). The 20 cm square format sealed tube detector [8] was developed by a collaboration (Large Area Picosecond Photon Detector - LAPPD) consisting of Incom. Inc., U. Chicago, Argonne National Laboratory, U. C. Berkeley, U. Hawaii, and several other institutions. These sealed tubes are intended for optical/UV imaging and timing applications in high energy physics, including detection of Cherenkov light (RICH), scintillation detection, and neutron imaging. The detector is a proximity focused device that is only ~20 mm thick with a UV transmissive input window. A semitransparent bialkali photocathode senses incoming light. Photoelectrons are then multiplied by a pair of 20 µm pore ALD borosilicate MCPs with a biased gap (1 mm), and there is a ~5 mm anode gap to a strip-line anode, or a resistive sheet anode. A number of sealed tubes have been successfully completed [22]. The bialkali photocathodes have good peak efficiency (30%) [22] and the uniformity was reasonably good for such a large area photocathode.

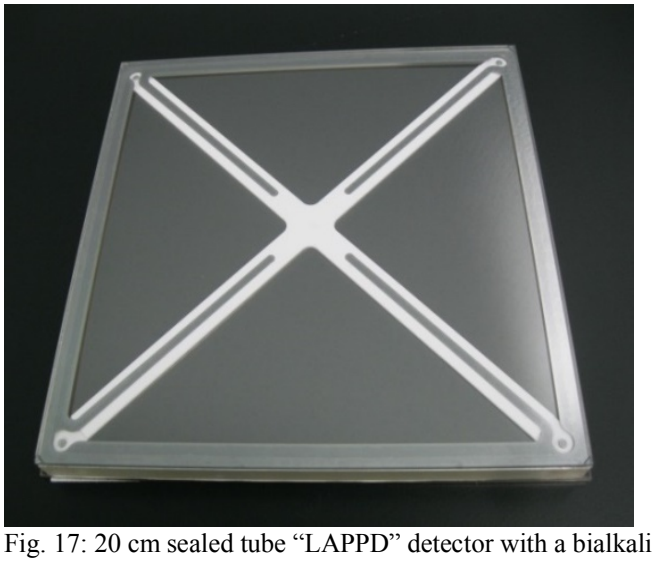

Fig. 17: 20 cm sealed tube "LAPPD" detector with a bialkali photocathode and 20 cm ALD borosilicate MCP pair (20µm pores, 60:1 l/d, 12° bias) with a resistive sheet anode.

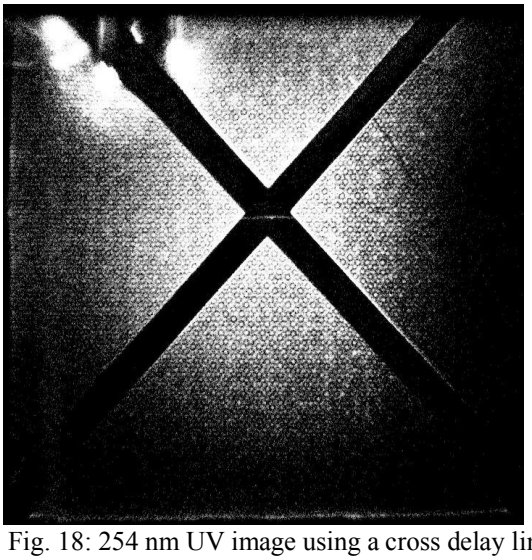

Fig. 18: 254 nm UV image using a cross delay line anode capacitively coupled to a LAPPD detector demonstrating imaging with ~ 100 µm resolution.

The strip anode has limited spatial resolution (~1 mm), but the high timing resolution it provides is appropriate for RICH applications. The event timing resolution of these large devices has been previously assessed [23] and shows a ~140 ps FWHM for single photoelectron events and <12 ps FWHM for large pulses. Adaptations of the LAPPD tube design with resistive anodes have also been made. A useful image readout scheme employs capacitive coupling of the resistive anode to an external 20 cm cross delay line anode for single event position encoding. The difference in signal arrival times at each end of two orthogonal delay lines allows photon positions in each axis to be determined, and the 400 cm^2 area cross delay line readout has an end to end signal propagation of ~130 ns. This detector scheme provides event by event accumulated images that can be used to characterize the spatial resolution of the 20 cm sealed tube. Using time to digital electronics with 12 bit electronic position coordinate binning, images were accumulated with a UV (254nm) illumination to directly stimulate the front surface of the MCPs. Although the illumination was not uniform the images clearly show the MCP multifiber pattern and the "X" mounting of the detector. Histograms of these features indicate that spatial resolution of ~100 μm FWHM has been achieved. Further iterations of this technique are in development to facilitate applications that require imaging fidelity while still preserving ~ns event timing capability.

7. ACKNOWLEDGEMENTS

We acknowledge the efforts of J. Hull, Dr. J. DeFazio, Photonis – (France & USA), and Incom Inc. for their assistance. This work was supported by NASA grants 80NSSC18K0291, NNX16AE92G & NNX14AD34G and DOE grant DE-SC0015267.

7. REFERENCES

[1] O. H. W. Siegmund, P. N. Jelinsky, S. R. Jelinsky, J. M. Stock, J. S. Hull, D. L. Doliber, J. Zaninovich, A. Tremsin, and K. E. Kromer, "High-resolution cross delay line detectors for the GALEX mission," *Proc. SPIE*, vol. 3765, pp. 429–440, 1999.

[2] J. Vallerga, J. Zaninovich, B. Welsh, O. H. W. Siegmund, J. McPhate, J. Hull, G. Gaines, and D. Buzasi, "The FUV detector for the cosmic origins spectrograph on the Hubble Space Telescope," *Nucl. Instr. Meth. Phys. Res. A*, vol. 477, no. 1, pp. 551–555, 2002.

[3] O. H. W. Siegmund, J. McPhate, A. Tremsin, J. Vallerga, B. Y. Welsh, and J. M. Wheatley, "High time resolution astronomical observations with the Berkeley Visible Image Tube," *AIP Conf. Proc.*, vol. 984, pp. 103–114, 2008.

[4] W. Priedhorsky and J. J. Bloch, "Optical detection of rapidly moving objects in space," *Appl. Opt.*, vol. 44, no. 3, pp. 423–433, 2005.

[5] O. H. W. Siegmund, J. Vallerga, P. Jelinsky, X. Michalet, and S. Weiss, "Cross delay line detectors for high time resolution astronomical polarimetry and biological fluorescence imaging," *IEEE Nucl Sci Conf R*, vol. 1, pp. 448–452, 2005.

[6] O. H. W. Siegmund, J. Vallerga, A. Tremsn, J. McPhate, and B. Welsh, "Optical Photon Counting Imaging Detectors with Nanosecond Time Resolution for Astronomy and Night Time Sensing," *Proc AMOS*, 2011.

[7] O. H. W. Siegmund, C. D. Ertley, S. R. Jelinsky, J. B. McPhate, J. Tedesco, M. J. Minot, A. O'Mahony, and C. A. Craven, "Very large area 20cm × 20cm flat panel phototubes using ALD microchannel plates," *Proc. IEEE NSS*, 2015, pp. 1–7.

[8] O. H. W. Siegmund, J. B. McPhate, S. R. Jelinsky, J. Vallerga, A. Tremsin, R. Hemphill, H. J. Frisch, R. G. Wagner, J. Elam, and A. Mane, "Large Area Microchannel Plate Imaging Event Counting Detectors with Sub-Nanosecond Timing," *IEEE Trans. Nucl. Sci.*, vol. 60, no. 2, pp. 923–931, 2013.

[9] C. Ertley, O. H. W. Siegmund, J. Schwarz, A. U. Mane, M. J. Minot, A. O'Mahony, C. A. Craven, and M. Popecki, "Characterization of borosilicate microchannel plates functionalized by atomic layer deposition," *Proc. SPIE*, vol. 9601, pp. 96010S–96010S–10, 2015.

[10] O. H. W. Siegmund, N. Richner, G. Gunjala, J. B. McPhate, A. Tremsin, H. J. Frisch, J. Elam, A. Mane, R. Wagner, C. A. Craven, and M. J. Minot, "Performance characteristics of atomic layer functionalized microchannel plates," *Proc. SPIE*, vol. 8859, p. 88590Y, 2013.

[11] Xie, J., "Photocathodes with VUV-UV-Vis full range response for fast timing and imaging applications," International Conference on High Energy Physics, 5 August 2016

[12] J. Vallerga, J. McPhate, A. Tremsin, O. H. W. Siegmund, R. Raffanti, H. Cumming, A. Seljak, V. Virta, and G. Varner, "Development of a flight qualified 100 x 100 mm MCP UV detector using advanced cross strip anodes and associated ASIC electronics," *Proc. SPIE*, vol. 9905, pp. 99053F–99053F–12. 2016.

[13] O. H. W. Siegmund, C. Ertley, J. Vallerga, E. Schindhelm, A. Harwit, B. Fleming, K. France, J. Green, S. R. McCandliss, and W. M. Harris, "Microchannel Plate Detector Technology Potential for LUVOIR," *Proc.*

SPIE. Vol. 10397, 1039711-8, 2017

[14] Photonis, "PLANACON™ Photodetector," https://www.photonis.com/en/product/planacon%E2%84%A2-photodetector. Jul. 2015.

[15] O. H. W. Siegmund, A. Tremsin, and J. Vallerga, "Development of cross strip MCP detectors for UV and optical instruments," *Proc. SPIE*, vol. 7435, pp. 74350L–74350L–10, 2009.

[16] J. Green, "Dual-channel Extreme Ultraviolet Continuum Spectrograph (DEUCE)," https://sites.wff.nasa.gov/code810/news/story209.html. [Online]. Available: https://sites.wff.nasa.gov/code810/news/story209.html. [Accessed: 14-Mar-2018].

[17] Ertley, C., O.H.W. Siegmund, T. Cremer, C. Craven, M. Minot, J. Elam, A. Mane. "Developments in atomic layer deposited microchannel plates". 1-7. 10.1109/NSSMIC.2016. 8069880C.

[18] O. Siegmund, C. Ertley, N. Darling, T. Curtis, J. Hull, J. Vallerga, C. Paw U, "Development of Sealed Tube Microchannel Plate Detectors with Cross Strip Readouts," IEEE Conf. Proc., N-07-047, 2018.

[19] Dorenbos, P., de Haas, J. T. M., Visser, R., van Eijk, C. W. E., Hollander, R. W., "Quantum efficiencies of several VUV-sensitive photomultiplier tubes," Nucl. Instr. Meth. Phys. Res. A **325**(1), 367–369 (1993).

[20] Araujo, H. M., Chepel, V. Y., Lopes, M. I., van der Marel, J., Marques, R. F., Policarpo, A. J. P. L., "Study of bialkali photocathodes below room temperature in the UV/VUV region," IEEE Trans. Nucl. Sci. **45**(3), 542–549 (1998)

[21] O. H. W. Siegmund, J. McPhate, H. Frisch, J. Elam, A. Mane, R. Wagner, and G. Varner, "Large Area Flat Panel Imaging Detectors for Astronomy and Night Time Sensing," *Proc. AMOS*, 2013.

[22] O. H. W. Siegmund, C. Ertley, J. V. Vallerga, T. Cremer, C. A., Craven, A. Lyashenko, M. J. Minot, "Single Photon Counting Large Format Imaging Sensors with High Spatial and Temporal Resolution," AMOS Conf. Proc., 2017.

[23] B. W. Adams, A. Elagin, H. J. Frisch, R. Obaid, E. Oberla, A. Vostrikov, R. G. Wagner, J. Wang, and M. Wetstein, "Timing characteristics of Large Area Picosecond Photodetectors," *Nucl. Instr. Meth. Phys. Res. A*, vol. 795, pp. 1–11, Sep. 2015.